The impacts of the hydraulic retention effect and typhoon disturbance on the carbon flux in shallow subtropical mountain lakes

Lin, Hao-Chi ; Tsai, Jeng-Wei ; Tada, Kazufumi ; Matsumoto, Hiroki ; Chiu, Chih-Yu ; Nakayama, Keisuke

(Citation)
Science of the Total Environment,803:150044

(Issue Date)
2022-01-10

(Resource Type)
journal article

(Version)
Version of Record

(URL)
https://hdl.handle.net/20.500.14094/90008655

Science of the Total Environment 803 (2022) 150044

Contents lists available at ScienceDirect

Science of the Total Environment

journal homepage: www.elsevier.com/locate/scitotenv

The impacts of the hydraulic retention effect and typhoon disturbance on the carbon flux in shallow subtropical mountain lakes

Hao-Chi Lin [a], Jeng-Wei Tsai [b], Kazufumi Tada [c], Hiroki Matsumoto [a], Chih-Yu Chiu [d,*], Keisuke Nakayama [a,*]

[a] Graduate School of Engineering, Kobe University, 1-1 Rokkodai-Cho, Nada-Ku, Kobe 658-8501, Japan
[b] Department of Biological Science and Technology, China Medical University, No. 100, Sec. 1, Jingmao Rd., Beitun Dist., Taichung City 406040, Taiwan
[c] Chuden Engineering Consultants, 2-3-30 Deshio, Minami-Ku, Hiroshima 734-8510, Japan
[d] Biodiversity Research Center, Academia Sinica, 128 Academia Road, Section 2, Nankang, Taipei 11529, Taiwan

HIGHLIGHTS

- Dissolved inorganic carbon (C) plays a crucial role in CO_2 emission.
- A 3D numerical model was used to estimate net ecosystem production.
- Typhoons and hydraulic retention control seasonal changes in dissolved inorganic C.
- A mesotrophic lake is a more substantial C sink than an oligotrophic lake.

GRAPHICAL ABSTRACT

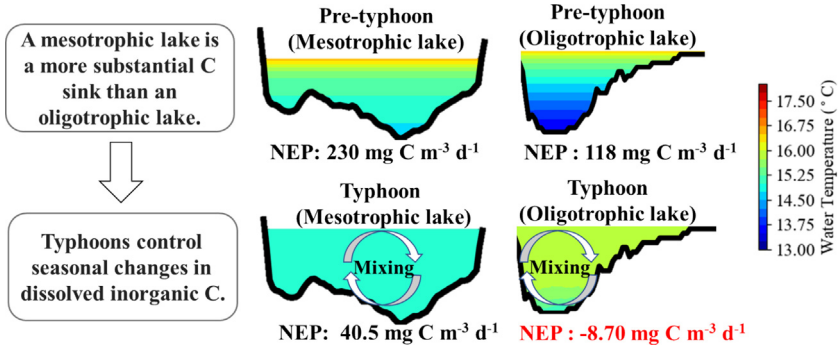

ARTICLE INFO

Article history:
Received 25 May 2021
Received in revised form 12 August 2021
Accepted 26 August 2021
Available online 3 September 2021

Editor: Ouyang Wei

Keywords:
Carbon flux
Net ecosystem production
Stratification
Residence time
Numerical simulation

ABSTRACT

A typhoon is extreme weather that flushes terrestrial carbon (C) loads and temporally mixes the entire water columns of lakes in subtropical regions. A C flux varies based on the trophic level associated with the ecological cycle related to hydraulic retention time (residence time). Herein, we sought to clarify how the hydraulic retention time and the disturbance from a typhoon affect the C flux regimes in two subtropical mountain lakes in a humid region of Taiwan with different trophic levels—oligotrophic and mesotrophic. We investigated the meteorological data and vertical profiles of the water temperature, dissolved inorganic carbon (DIC), dissolved organic C (DOC), and chlorophyll *a* (Chl. *a*) during the pre-typhoon period (April–July), during the typhoon period (August–November), and the post-typhoon period (December–March) for five years (2009–2010 and 2015–2017). We applied a three-dimensional environmental model (Fantom) to investigate the hydraulic retention effect on the net ecosystem production (NEP) using the residence time in stratified lakes. The results demonstrate that typhoon-induced mixing associated with the hydraulic retention effect plays one of the critical roles in controlling the NEP and C flux in shallow subtropical lakes.

1. Introduction

Physical and hydrological processes are vital to understanding carbon (C) flux responses in lake ecosystems under climate change-induced extreme weather events (Woolway et al., 2018, 2020). The vertical mixing of water columns by the wind affects mainly small lake ecosystems (surface area < 1 km^2 and average water depth < 15 m)

* Corresponding authors.
E-mail addresses: bochiu@sinica.edu.tw (C.-Y. Chiu), nakayama@phoenix.kobe-u.ac.jp (K. Nakayama).

https://doi.org/10.1016/j.scitotenv.2021.150044

rather than deep and large lake ecosystems. For example, wind-induced mixing (MacIntyre et al., 2018) and storms (Vachon and del Giorgio, 2014; Czikowsky et al., 2018) quickly induce vertical disturbance in small lakes. Intense precipitation and strong wind during typhoons enhance the mixing of shallow lakes in subtropical regions (Tsai et al., 2011; Kimura et al., 2014, 2017). Typhoons produce intensive precipitation, ranging from 200 mm d^{-1} to 1000 mm d^{-1} (Tsai et al., 2011; Kimura et al., 2012) and contribute >50% of the annual rainfall in subtropical regions (Tsai et al., 2008, 2016; Chiu et al., 2020). However, it is not yet clear how typhoons influence the mixing regimes and biogeochemical processes of subtropical lakes (Kimura et al., 2012, 2014, 2017; Tsai et al., 2008, 2011; Chiu et al., 2020).

Dissolved organic C (DOC) plays a vital role in the C flux in freshwater ecosystems, and DOC regulates the lake metabolism of shallow subtropical lakes (Tsai et al., 2008, 2016). DOC has been recognized globally to be a significant modifier of lake ecosystem structures and functions, serving as a substrate for microbial photosynthesis/respiration (Tranvik, 1988) within lakes, catchment hydrology, and terrestrial vegetations (Sobek et al., 2005). Sobek et al. (2005) demonstrated a positive relationship between the partial pressure of CO_2 (pCO_2) and DOC. Colored dissolved organic C (CDOC) reduces the ultraviolet radiation (UVR) and photosynthetically active radiation (PAR) (400 nm–700 nm) that penetrates the water body, and this may push the ecosystem towards heterotrophic primary production but enhance the thermal-strength stratification (Scully et al., 1996; Williamson et al., 1999; Anesio and Granéli, 2003; Read and Rose, 2013; Rose et al., 2016; Bartosiewicz et al., 2019). Allochthonous and autochthonous DOC is transported to the lakes, affecting the lake C flux through rainstorms, drought, browning, mineralization, and acidification via sediment, rivers, and groundwater (den Heyer and Kalff, 1998; Schindler et al., 1996; Anesio and Granéli, 2003; Sobek et al., 2007; Ojala et al., 2011; Williamson et al., 2015; Chiu et al., 2020). Mineralization (or photochemical mineralization) is one of the most critical processes affecting the production CO_2 (Groeneveld et al., 2016; Vachon et al., 2017; Bartosiewicz et al., 2019; Allesson et al., 2020). DOC is thus expected to be highly correlated with the C flux (Hope et al., 1994, 1996; Sobek et al., 2003, 2005).

Dissolved inorganic C (DIC) is principally associated with the pCO_2 to obtain CO_2 emissions across the air-water interface if the calcification is negligible within a lake (Smith, 1985; Striegl et al., 2001; Bade et al., 2004). A sink of DIC in a lake includes river inflows from terrestrial ecosystems, autotrophic organism production (photosynthesis), and sediment (Hope et al., 1994; Cole et al., 2007; Vachon and del Giorgio, 2014; Dodds and Whiles, 2020). Changes in the wind speed, thermal stratification, and water quality change the vertical distribution of DIC in a lake (Cole and Caraco, 1998; Sobek et al., 2005; McDonald et al., 2013; Czikowsky et al., 2018; Lin et al., 2021). The net ecosystem production (NEP) is defined as the gross primary production (GPP) minus the ecological respiration (ER) within the ecosystem. Generally, in a shallow subtropical lake, the GPP is greater than the ER within the upper layer (epilimnion) due to stratification from spring to summer, showing a low level of DIC in the epilimnion (Lin et al., 2021). The stratification inhibits the vertical mixing of DIC between the upper and lower layers, resulting in the high concentration of DIC in the hypolimnion (Lin et al., 2021). In contrast, the vertical mixing is enhanced due to typhoons or turnover from autumn to winter, following the vertically uniform DIC profile. In the investigation of an oligotrophic lake by Lin et al. (2021), both the GPP and ER were low, and Lin et al. observed that the values of the CO_2 emission across the water surface into the atmosphere were positive all year round.

Pulse river loadings induced by typhoon precipitation export a large amount of terrestrial organic C into shallow subtropical lakes during monsoon and typhoon seasons (spring to autumn) (Tsai et al., 2008, 2016; Chiu et al., 2020). The strength and frequency of typhoons were shown to determine the CO_2 flux and lake metabolism in shallow subtropical lakes (Jones et al., 2009; Tsai et al., 2011). We thus hypothesized that temporal and spatial variations in DOC and DIC are affected by physical factors such as the vertical mixing, water flushing, and residence time during the typhoon season. These factors might influence the primary production and nutrient levels in lakes, especially under changing precipitation patterns (Woolway et al., 2018; Chiu et al., 2020; Nakayama et al., 2020a; Lin et al., 2021). We conducted the present study to (*i*) clarify how typhoon disturbance impacts the C flux, paying particular attention to the effects of the inflow and stratification on the CO_2 flux in shallow lakes with different trophic levels; and (*ii*) estimate the NEP using a three-dimensional (3D) environmental model to simulate a stratified lake's hydraulic retention effect.

2. Materials and methods

2.1. Study sites

This study was conducted in two subtropical mountain lakes in a humid region of Taiwan (Fig. 1) with high precipitation (>3000 mm per year) (Lai et al., 2006). Typhoon events contribute roughly 50% of the annual rainfall in that region (Tsai et al., 2008, 2016; Chiu et al., 2020). The daily water surface (epilimnion) temperature ranges from 5.0 °C to 25 °C (Chiu et al., 2020). The daily average air temperature is approx. 15 °C to 25 °C, and stratification occurs from March to November. The water column mixes from December to February (Lai et al., 2006; Kimura et al., 2012, 2017; Chiu et al., 2020; Lin et al., 2021). The typhoon season in Taiwan is from August to November (Tsai et al., 2011; Kimura et al., 2012).

Yuang-Yang Lake (YYL) is located in the Chilan mountain region at around 1650 m asl (24.58° N, 121.40° E). YYL has six inflows, one outflow, a surface area of 0.035 km^2, and an average total water depth of 4.3 m. It is a humic lake with brown-colored water (Tsai et al., 2008). The lake's chlorophyll *a* (Chl. *a*) concentration is <5.0 μg L^{-1} at the surface layer (0.04 m–0.25 m deep). Regarding the nutrient levels, total phosphorous (TP) ranges from 10 μg-P L^{-1} to 20 μg-P L^{-1}, and total nitrogen (TN) ranges from 20 μg-N L^{-1} to 50 μg-N L^{-1} (Tsai et al., 2008; Chiu et al., 2020). The seasonal variation in the lake's NEP ranges from −11.4 μmol to −74.9 μmol of O_2 m^{-3} d^{-1} (Tsai et al., 2008). YYL is thus considered a typical oligotrophic lake.

Tsui-Fong Lake (TFL) is located on Taiping Mountain at around 1850 m asl (24.52° N, 121.60° E) and has 11 inflows (one primary and ten minor flows) (Fig. 1). Shale cracks are the only outflow, and there is no river outflow in the watershed. The lake's surface area varies from 0.08 km^2 to 0.25 km^2, and the total water depth ranges from 3.0 m during the dry period to 12 m during typhoon season (Tsai et al., 2016; Chiu et al., 2020). The average total water depth is 4.2 m. The watercolor of TFL is green during the dry period due to algal blooms between March and June, with the high Chl. *a* of 30 μg L^{-1}. TP and TN are around 30–60 μg-P L^{-1} and 20–70 μg-N L^{-1}, respectively, indicating that TFL is mesotrophic (Tsai et al., 2016; Chiu et al., 2020). The lake's NEP values range from −25.4 μmol in winter to 57.4 μmol of O_2 m^{-3} d^{-1} in spring in the typical year (Chiu et al., 2020). TFL is thus considered a typical mesotrophic lake.

2.2. Data collection and measurements

We collected the meteorological and water quality data of the two lakes from 2009 to 2010 and 2015 to 2017 (5 years total). Given that the thermal regime conditions of lakes' water columns are affected by typhoon conditions (Lin et al., 2021), we categorized the seasonal pattern into three periods and observed that the C adjacent to the water surface tends to be higher during the typhoon season. Therefore, to determine how water quality variables (DOC, DIC, Chl. *a*) differ between before and after typhoons, we categorized the seasonal pattern into three periods: 'pre-typhoon' (April to July), 'during-typhoon' (August to November), and 'post-typhoon' (December to March). We created a high-resolution water quality dataset of monthly values of DOC, DIC, pH, and Chl. *a* in YYL and TFL for 5 years, enabling us to investigate

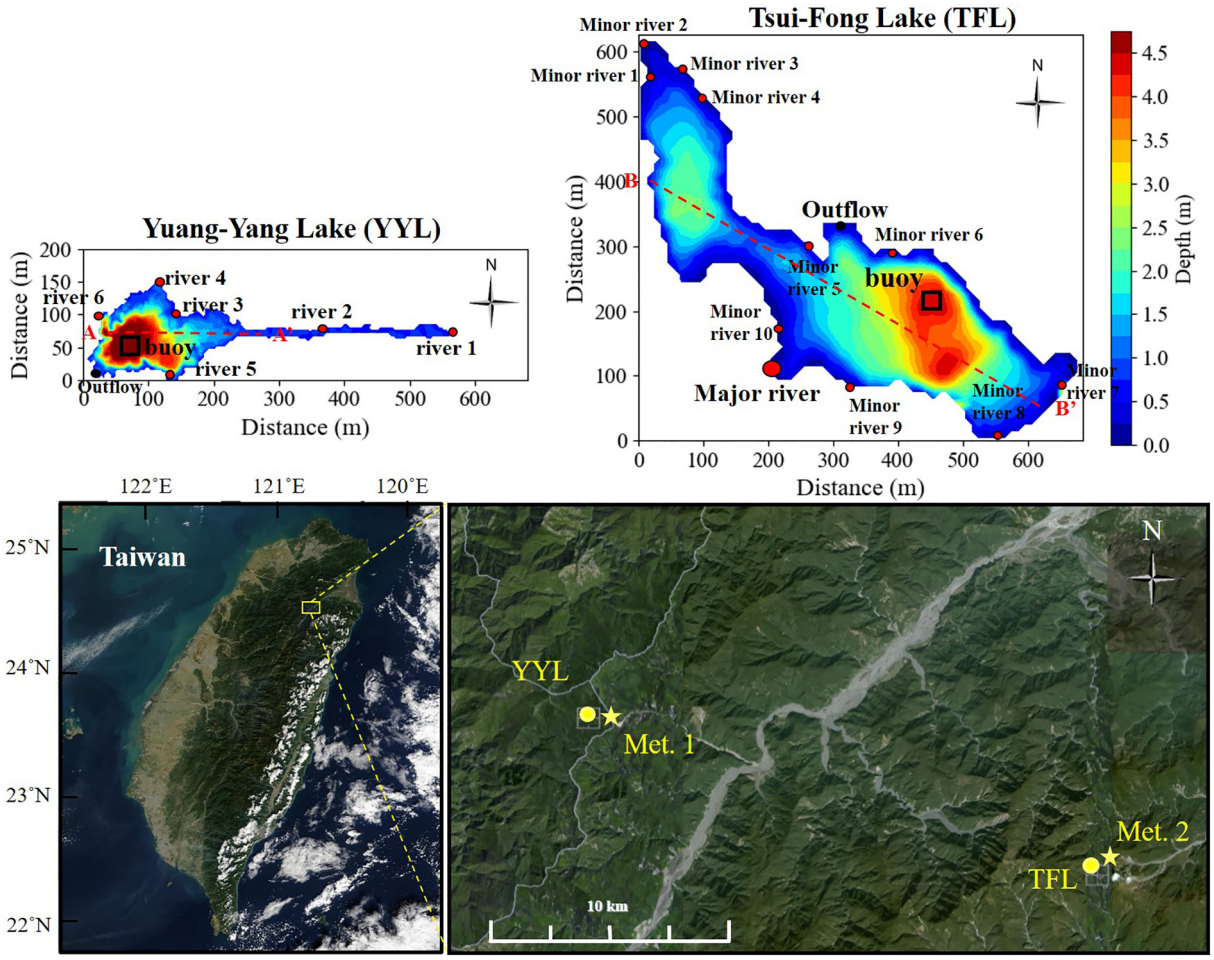

Fig. 1. Location of sites with an enlarged bathymetric map of Yuan-Yang Lake (YYL) and Tsui-Fong Lake (TFL) with the water-depth contour. Buoys (*black rectangles*), weather stations (*stars*, Met. 1 and Met. 2) and the river inflow (*red circles*) and outflow (*black dots*) deployment sites are shown. The satellite images are from MODIS Rapid Response Team, NASA (*left*), and Google Earth (*right*). A-A′ and B-B′ indicate the vertical cross-section shown in Suppl. Fig. S5. (For interpretation of the references to color in this figure legend, the reader is referred to the web version of this article.)

the changes in the C flux in the pre-typhoon, during-typhoon, and post-typhoon periods.

2.2.1. Meteorological and limnological data

We deployed buoys at the deepest spot of both lakes to measure the wind speed and wind direction 2.0 m above the water surface using wind monitors (model 03001, R.M. Young, Traverse, MI, USA). The water depths were measured every 1.0 m through the water column by a water depth meter (model HOBO U20; Onset Computer Corp., Bourne, MA), and the water temperature was measured at water depths of 0.04, 0.25, 0.50, 1.00, 2.00, and 3.50 m with the use of thermistor chains (Templine, Apprise Technologies, Duluth, MN). Daily precipitation was recorded using a tipping bucket rain gauge (model N-68; Nippon Electric Instrument, Tokyo). The air pressure (model 090D; Met One Instruments, Grants Pass, OR) and the photosynthetically active radiation (PAR) (model LI-190; LI-COR, Lincoln, NE) were measured using sensors at weather stations located ~1.0 km from the buoys (Fig. 1). The measured data were automatically saved every 10 min in a data logger (model CR1000, Campbell Scientific, Logan, UT) at each buoy and weather station.

2.2.2. Water chemical samples (DIC, DOC, and Chl. a)

We collected water samples for the analysis of DIC, DOC, and Chl. *a* at water depths of 0.04, 0.50, 1.00, 2.00, and 3.50 m at the buoy sites using a horizontal Van Dorn bottle (2.20 L, acrylic). The pH was measured using a water quality probe (model Hydrolab 4α; Hach, Loveland, CO) at 0.04 m deep (epilimnion). We also sampled surface water from river inflows and outflows (Fig. 1). The samples were filtered (47 mm GF/F, nominal pore size 0.70 μm, Whatman, Maidstone, Kent, UK) using a portable hand pump (Hand Vacuum pump, Lincoln Industrial Corp. *St.* Louis, MO). The filter papers were kept in opaque bottles in a refrigerator at −25 °C until Chl. *a* was extracted from the filter papers with methanol.

The extracts of filter paper were then measured by a portable fluorometer (model 10-AU-005-CE; Turner Designs, Sunnyvale, CA) to obtain the Chl. *a* concentration. The filtrated samples were kept in airtight vials (Vial glass, 40-mL, #K60958A-912, Kimble) stored in an icebox at approx. 4 °C until the DIC and DOC concentrations were analyzed using a total organic carbon (TOC) analyzer (model 1030W/1088, Xylem, TX). An infrared gas detector detected DOC and DIC with persulfate digestion. These samples were analyzed <72 h after sampling. The Chl. *a* and colored dissolved organic matter (CDOM) were measured at 0.25 m deep and saved automatically using a Submersible Fluorometer (model C3, Turner Designs) every 10 min.

2.3. Data analysis

To clarify the seasonal differences in water quality between the epilimnion and hypolimnion, we used the DIC, DOC, and Chl. *a* values from water depths of 0.04 to 3.50 m. The epilimnion DIC, meteorological data (wind speed, air pressure), and limnological (pH, water temperature) were used to calculate both the CO_2 flux between the lakes and

atmosphere as described below in Section 2.3.1 and the NEP using a residence time as shown in Section 2.3.2. We applied structure equation model (SEM) to quantify the influence of the meteorological and water quality variables on the DIC flux (Suppl. File 1). We also performed hydrological model simulations to evaluate the effect of typhoon disturbance on the DIC residence time within the two lakes.

2.3.1. The CO_2 flux between the lake surface water and atmosphere (F_{CO2})

The NEP is associated with the following physical and hydrological processes on C flux: the river inflow and outflow DIC, the CO_2 flux from the bottom sediment, and the CO_2 flux across the air-water interface (Lin et al., 2021). We thus applied Fick's law to obtain the CO_2 flux between the lake surface water and atmosphere (F_{CO2}) (mg CO_2 m^{-2} d^{-1}) by using the following equation:

$$F_{CO2} = k_{CO2} \cdot K_H(pCO2_{water} - pCO2_{air}) \quad (1)$$

where k_{CO2} is the gas transfer velocity, K_H is the Henry's coefficient, $pCO2_{air}$ (μatm) is the CO_2 partial pressure in the atmosphere (air pressure [atm] = 400 [ppm]), and $pCO2_{water}$ (μatm) is the CO_2 partial pressure in the water, which is determined as follows (Smith, 1985; Cai and Wang, 1998):

$$pCO2_{water} = \frac{DIC\left(10^{-pH}\right)^2}{\left[\left(10^{-pH}\right)^2 + \left(10^{-pH}\right)K_1 + K_1K_2\right]K_H} \quad (2)$$

where *DIC* is the DIC concentration at 0.04 m water depth, K_1 is the 1st dissociation constant, and K_2 is the 2nd dissociation constant for DIC. K_H, K_1, and K_2 are determined by the following empirical equations using the water temperature (K) as follows (Plummer and Busenberg, 1982):

$$K_H = \exp\left(108.39 + 0.0199\mathrm{T} - \frac{6920}{\mathrm{T}} - 40.452\log\mathrm{T} + \frac{669365}{T^2}\right) \quad (3)$$

$$K_1 = \exp\left(-356.31 - 0.0609\mathrm{T} + \frac{21834}{\mathrm{T}} + 126.83\log\mathrm{T} - \frac{1684915}{\mathrm{T}^2}\right) \quad (4)$$

$$K_2 = \exp\left(-107.8 - 0.0325\mathrm{T} + \frac{5152}{\mathrm{T}} + 38.926\log\mathrm{T} - \frac{56371}{T^2}\right) \quad (5)$$

K_{CO2} (Smith, 1985; Jähne et al., 1987) is:

$$K_{CO2} = k_{600}\left(\frac{Sc_{CO_2}}{600}\right)^{-0.5} \quad (6)$$

where Sc_{CO2} is the Schmidt number from the following empirical equation (Wanninkhof, 1992):

$$Sc_{CO2} = 1911.1 - 118.11\,T + 3.4527\,T^2 - 0.04132\,T^3 \quad (7)$$

and K_{600} is the gas exchange coefficient shown as follows (Cole and Caraco, 1998):

$$K_{600} = 2.07 + 0.215\,U_{10}^{1.7} \quad (8)$$

$$U_{10} = U_2 \cdot \left(\frac{10_{(m)}}{2_{(m)}}\right)^{0.15} \quad (9)$$

where U_2 is the wind speed at 2.00 m above the lake surface.

2.3.2. Residence time and the NEP

Lin et al. (2021) revealed that the residence time should be estimated using a 3D numerical model that enables analyses of the effect of stratification on mass transport when the hydraulic retention is strongly associated with the NEP. We thus applied a 3D environmental model (Fantom) to estimate the residence time (t_r) (Nakayama et al., 2020a; Lin et al., 2021). Fantom is based on object-oriented programming methods that consider bathymetry data (Nakamoto et al., 2013; Nakayama et al., 2014, 2016, 2020b), and we used a generic length-scale equation model to perform the water mass and energy transport calculations (Jones and Launder, 1972; Umlauf and Burchard, 2003).

To consider the bottom slopes within lakes, we created a Fantom to simulate a z-coordinate system with partial cells (Adcroft et al., 1997). The lake bathymetry was measured using sonar (model LMS-332c GPS Receiver and Sonar, Lowrance, USA) in August 2007 every 1.00 m in depth. For numerical simulations, the horizontal grid size was 4.00 m in YYL and 10.0 m in TFL. The vertical grid size was 0.20 m, and the time step was 0.50 s in both lakes. We used the base inflows at the river flows and outflows (Fig. 1). The average base inflows were 0.185 (pre-typhoon), 0.411 (during-typhoon), and 0.067 m^3 s^{-1} (post-typhoon) in TFL, and 0.048, 0.107, and 0.028 m^3 s^{-1} in YYL, respectively. The vertical profiles of average water temperature are presented herein as the initial conditions in each period. The initial water depths were 3.27 (pre-typhoon), 7.01 (during-typhoon), and 4.08 m (post-typhoon) in TFL, and 4.38, 4.46, and 4.35 m in YYL for each period, respectively.

The residence time, t_r, of a lake is calculated by dividing the lake volume by the mean rate of inflow, which plays a critical factor in evaluating the C flux and ecosystem function. In practice, the actual t_r is not equal to (lake volume)/(inflow discharge) because the stratification affects the three-dimensional flow and mass transport. We therefore applied Fantom to estimate t_r from the temporal change in tracer concentrations using Fantom (Nakayama et al., 2020a; Lin et al., 2021). We first used a uniform tracer concentration of 1.0 for the entire domain of each lake, and we then computed the time series of the mean tracer concentration, which we used to estimate the residence time using the equation:

$$Tr = (Tr_0 - Tr_L)\exp\left(-\frac{t}{t_r}\right) + Tr_L \quad (10)$$

where *Tr* is the average tracer concentration in the entire available computational domain, Tr_0 (=1.0 unit) is the initial tracer concentration, *t* is the time, and Tr_L is the quasi-steady-state tracer concentration.

Tr_L tends to be 0 when there is no stratification and >0 in a stratified lake. The larger the lower-layer volume, the shorter the Tr_L. Thus, Tr_L indicates the effect of stratification on the hydraulic retention time.

The NEP (mg C m^{-3} d^{-1}) was modeled by applying the following conceptual model (Nakayama et al., 2020a; Lin et al., 2021):

$$\mathrm{NEP} = \frac{C_U(\mathrm{DIC}_R - \mathrm{DIC}_L)}{t_r} - \frac{A_L}{V_{total}}F_{CO2} \quad (11)$$

where DIC_R is the average river DIC (mg C L^{-1}), DIC_L is the average vertical profile of DIC, A_L is the lake surface area (m^2), C_U is the coefficient that converts the unit from mg C L^{-1} to mg C m^{-3}, V_{total} is the total lake volume (m^3), and F_{CO2} is the CO_2 emission across the air-water interface (mg C m^{-2} d^{-1}), as described above in Section 2.3.1.

3. Results

3.1. The seasonal dynamics of the metrological and limnological data

In YYL, the average total water depth was 4.40 m between 2009 and 2017 (Fig. 2a). The average wind speed was 1.07 m s^{-1}, and the maximum wind speed exceeded 8.0 m s^{-1} during typhoons (Fig. 2a). The daily epilimnion temperatures ranged from 5.60 °C to 23.9 °C (Fig. 2b). The vertical profile of the water temperature showed stratification from April to September (around day of the year [DOY] 92 to DOY 245) and a well-mixed water column from December to February (~DOY 335 to the next year's DOY 59) (Fig. 2b). The average epilimnion DIC was 2.42 mg C L^{-1}, ranging from 0.50 to 7.06 mg C L^{-1} (Fig. 2c). In

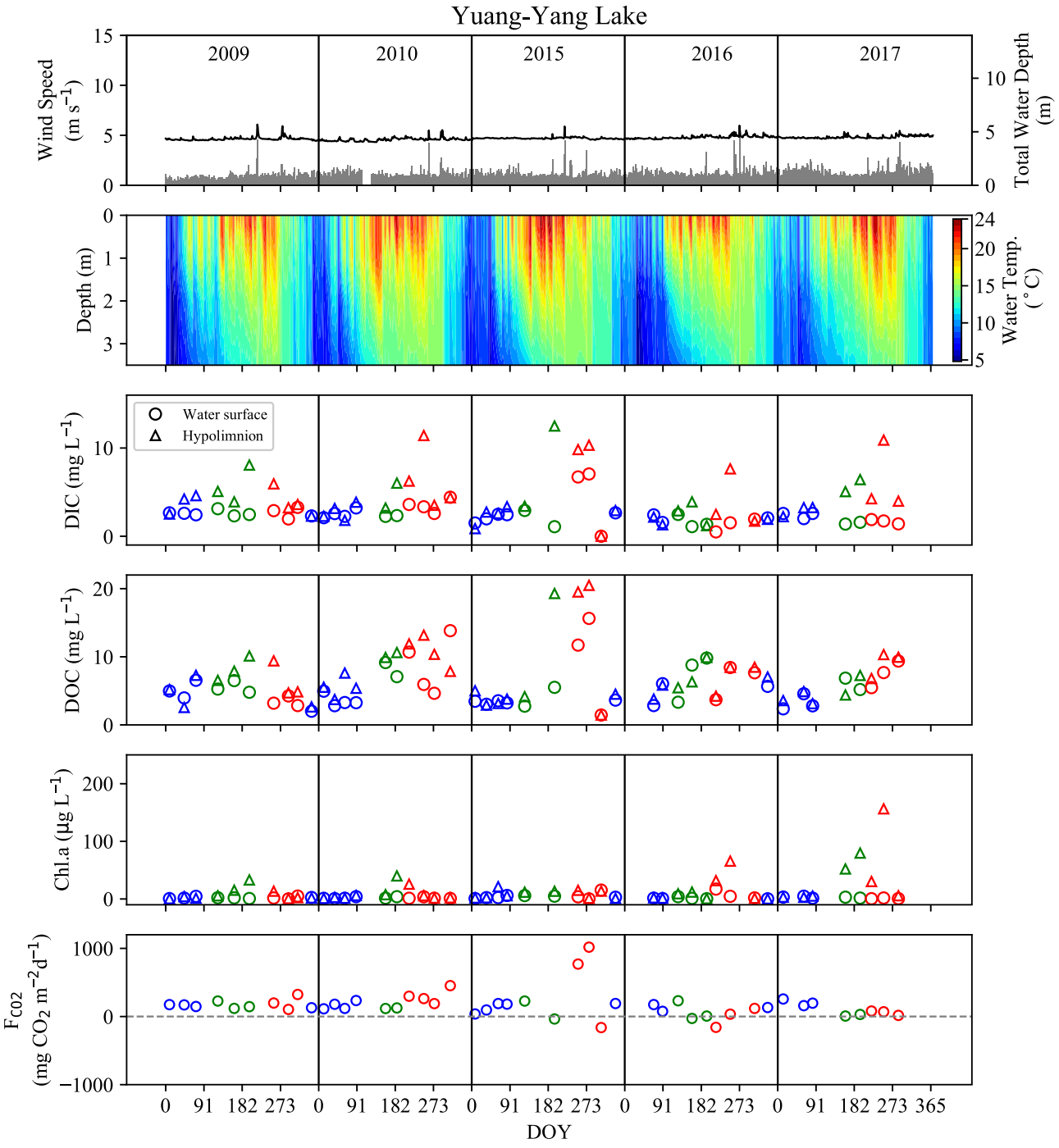

Fig. 2. Five years of temporal data on (a) wind speed (U_{10}, *gray bars*) and total water depth (*solid black line*), (b) water temperature, (c) DIC, (d) DOC, (e) the Chl. *a* at the water surface (*hollow circles*) and the hypolimnion at 3.50 m water depth (*hollow triangles*), and (f) the C emission across the airwater interface (F_{CO2}) in YYL. (a–b) are daily averages and (c–f) are water samplings per month in the pre-typhoon period (*green*), during-typhoon period (*red*), and post-typhoon period (*blue*). DOY: the day of the year. (For interpretation of the references to color in this figure legend, the reader is referred to the web version of this article.)

June, the maximum hypolimnion DIC was 10.3 mg C L^{-1}, which is approximately ten times higher than the maximum epilimnion. The DIC was not significantly different between the epilimnion and hypolimnion from December to January (around 335 to the next 31 DOY).

The average epilimnion and hypolimnion DOC were 5.63 and 7.26 mg C L^{-1}, respectively (Fig. 2d). The DOC was approx. two times higher than the DIC concentration (Fig. 2c, d). The DOC and DIC were approx. two to ten times higher during typhoon periods (August to November) than the other periods (Fig. 2c, d). The average epilimnion Chl. *a* was 2.92 μg L^{-1}. The hypolimnion Chl. *a* was two to ten times higher (around 30.0 μg L^{-1}–150 μg L^{-1}) than the epilimnion Chl. *a* due to the algal bloom from April to August (Fig. 2e). YYL was found to release C into the atmosphere (Fig. 2f). The average F_{CO2} was 165 mg CO_2 m^{-2} d^{-1}, ranging from −163 mg to 1018 mg of CO_2 m^{-2} d^{-1} (Fig. 2f). Overall, the water quality (DIC, DOC, Chl. *a*) and F_{CO2} were higher during the typhoon period compared to the pre-typhoon and post-typhoon periods (Fig. 2c–f).

In TFL, the average and the total water depth variation were higher than those of YYL because TFL had only seepage flow and no significant river outflow. However, the watershed flowing into TFL was larger than

that flowing into YYL, and the maximum water depth was >10.0 m. Therefore, the total water depth returned to the average value of 30.0 d or more after a typhoon (Fig. 3a). In addition, the daily wind speeds in TFL are higher than those in YYL (Figs. 2a, 3a). The maximum wind speed at TFL was 14.7 m s^{-1} during the typhoon. The average wind speed at TFL was 1.89 m s^{-1} and significantly higher than that at YYL. The average epilimnion temperature in TFL was 15.8 °C (Fig. 3b). The maximum water temperature in TFL was 25.5 °C, with a difference of 8.0 °C between the epilimnion and hypolimnion on July 5, 2010. Apparently, the mixing depth in TFL is deeper than that in YYL because of the slightly stronger wind at TFL.

However, measuring the hypolimnion water temperature from the thermistor chain after rains was impossible because the total water depth was greater than the thermistor's length (3.50 m). The epilimnion DIC value in TFL was approx. 0.50 mg–7.00 mg C L^{-1} (Fig. 3c), and the average epilimnion DOC and hypolimnion DOC values were 4.40 and 4.62 mg C L^{-1}, respectively (Fig. 3d). The average epilimnion Chl. *a* in TFL was 43.9 μg L^{-1}, which was higher than that of YYL, and the maximum Chl. *a* was 153 μg L^{-1} (Fig. 3e). The F_{CO2} in TFL ranged from −0.17 mg to −361 mg of CO_2 m^{-2} d^{-1} (excluding July to October 2015 and August 2016), which indicated that TFL is a C sink (Fig. 3f). Overall, the water quality and absolute value of F_{CO2} were higher in

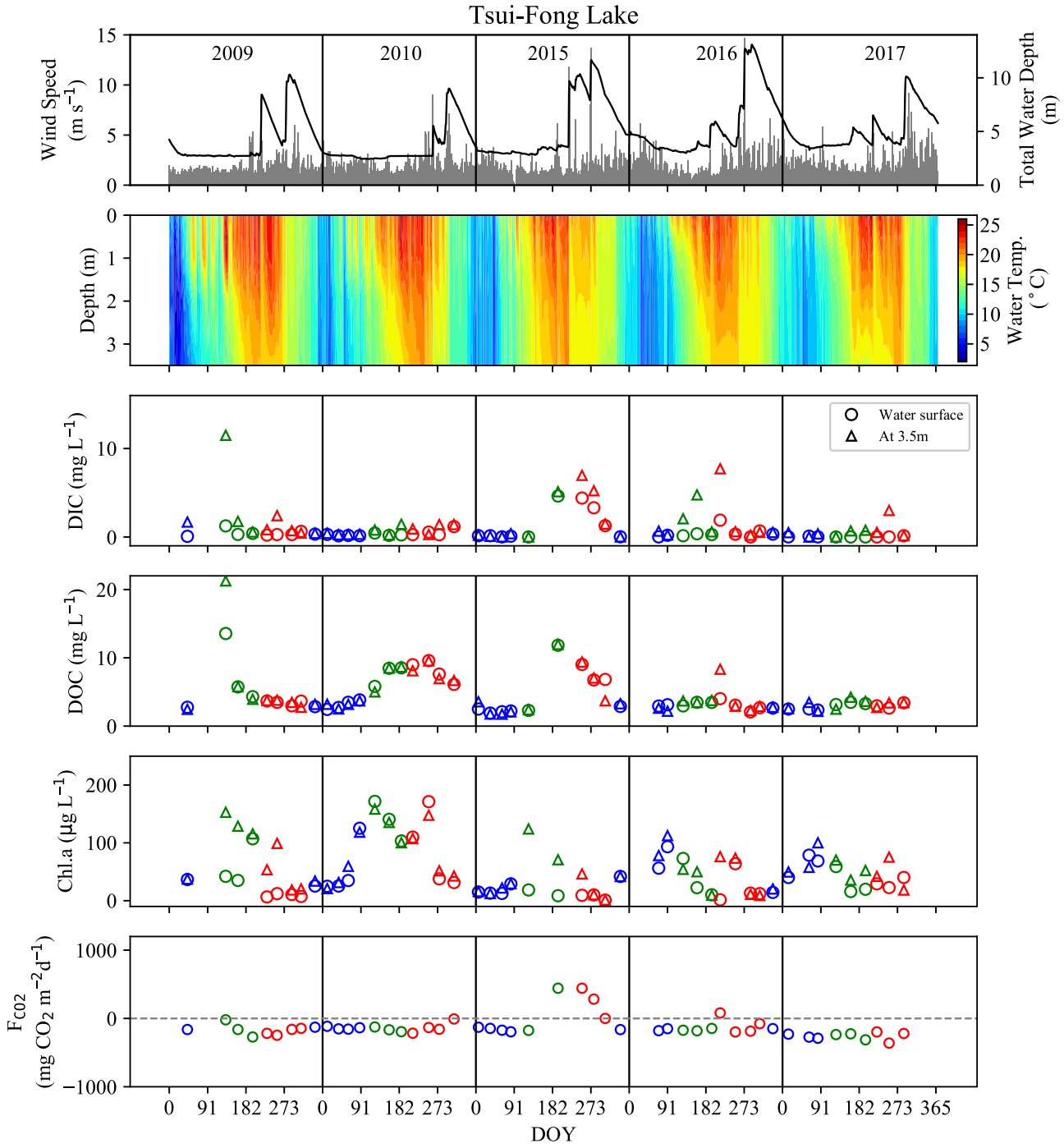

Fig. 3. Five years of temporal data on (a) wind speed (U_{10}, *gray bars*) and total water depth (*solid black line*), (b) water temperature, (c) DIC, (d) DOC, (e) the Chl. *a* at the water surface (*hollow circles*) and at 3.50 m water depth (*hollow triangles*), and (f) the C emission across the air-water interface (F_{CO2}) in TFL. (a–b) Daily averages and (c–f) water samplings per month in the pre-typhoon period (*green*), during-typhoon period (*red*), and posttyphoon period (*blue*). (For interpretation of the references to color in this figure legend, the reader is referred to the web version of this article.)

the pre-typhoon period due to the algal bloom and were diluted during the typhoon (Fig. 3c–f).

3.2. Variations in water temperature, DIC, Chl. a, and NEP during the pre- and post-typhoon periods

The average epilimnion temperatures during the pre- and during-typhoon periods were 19.5 °C and 19.2 °C in TFL and 18.0 °C and 17.9 °C in YYL (Fig. 4a, b), respectively. In the post-typhoon period, the average epilimnion temperature was 12.6 °C in TFL and 12.7 °C in YYL (Fig. 4a, b). Overall, the measured epilimnion DIC was higher in the during-typhoon period than the pre- and post-typhoon periods in both lakes, at 0.71 mg C L^{-1} (average pre- and post-typhoon) and 0.88 mg C L^{-1} (during-typhoon) in TFL and 2.91 mg C L^{-1} and 6.01 mg C L^{-1} in YYL at 3.50 m water depth, respectively (Fig. 4c, d). The average Chl. *a* was relatively constant at the epilimnion in YYL (Fig. 4e), whereas in TFL the

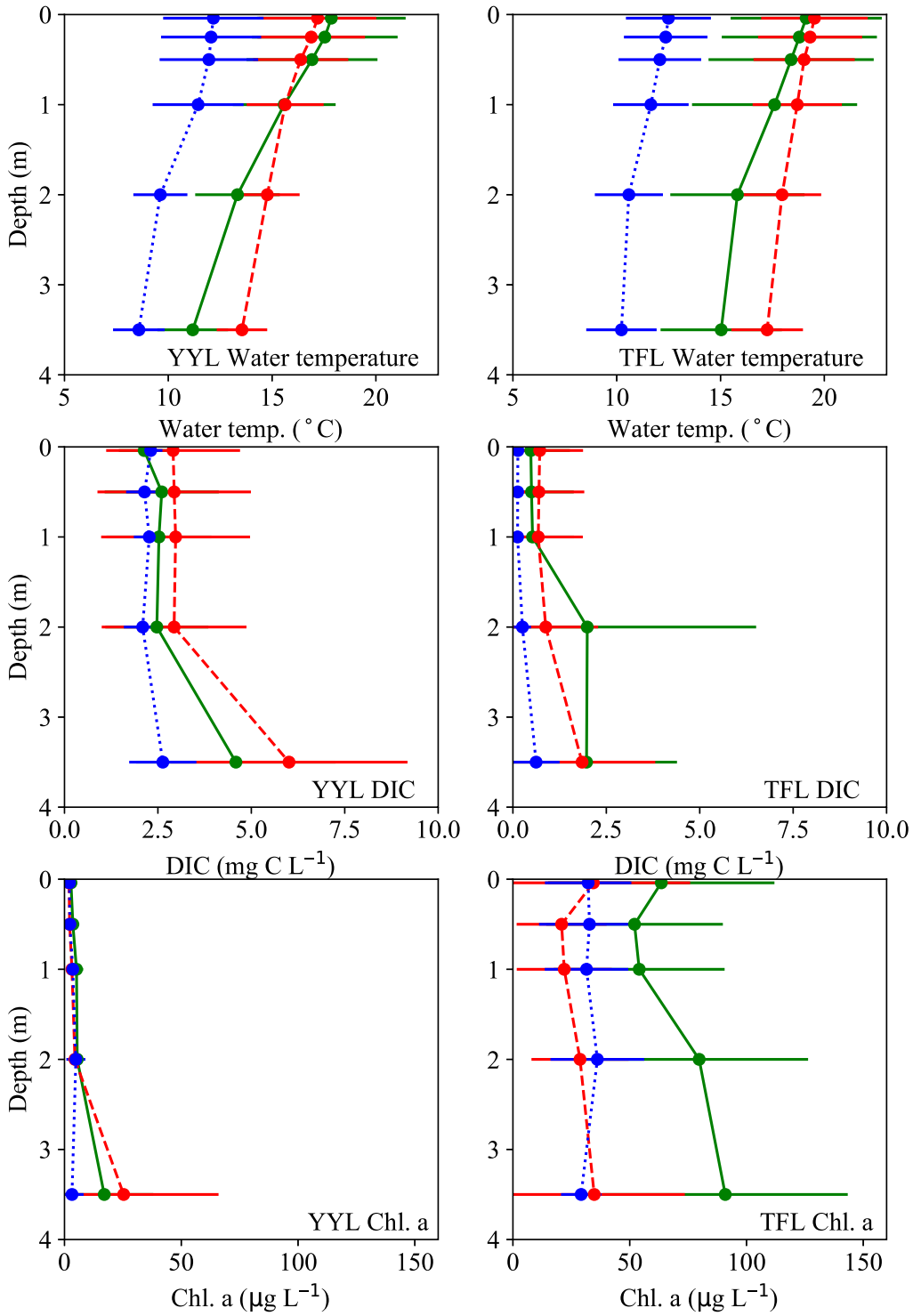

Fig. 4. Vertical profiles of average (a, b) water temperature, (c, d) DIC, and (e, f) Chl. *a* and DIC in the pre-typhoon period (*solid green lines*), during-typhoon period (*red dashes*), and post-typhoon period (*blue dotted lines*) from January 2009 to December 2017 within the lakes. The *dots* and *crosses* show the average value, and the *horizontal lines* indicate the standard deviation (SD). (For interpretation of the references to color in this figure legend, the reader is referred to the web version of this article.)

average Chl. *a* changed from 63.5 μg L^{-1} (pre-typhoon) to 34.8 μg L^{-1} (during-typhoon) at the epilimnion (Fig. 4f). Chl. *a* decreased from 90.9 μg L^{-1} (pre-typhoon) to 34.2 (during-typhoon) μg L^{-1} at 3.50 m water depth in TFL (Fig. 4f).

The numerical simulation results showed that the residence time (t_r) was 5.80 d (pre-typhoon), 4.40 d (during-), and 5.70 d (post-typhoon) in YYL, indicating that the hydraulic retention time is less than the 1-week period that phytoplankton need to grow. In contrast, the residence times of TFL were 10.0 d (pre-typhoon), 18.0 d (during-), and 39.0 d (post-typhoon), which were longer than those of YYL (Table 1). As a result, C was absorbed into both lakes during the pre-typhoon period, as the NEP was 230 mg C m^{-3} d^{-1} in TFL and 118 mg C m^{-3} d^{-1} in YYL (Fig. 5). However, the NEP in YYL was negative: −8.70 mg C m^{-3} d^{-1} and −42.1 mg C m^{-3} d^{-1} in the during- and post-typhoon periods, respectively. In TFL, the NEP was 97.3 mg m^{-3} d^{-1} in the during-typhoon period and 40.5 mg C m^{-3} d^{-1} in the post-typhoon period. The high Chl. *a* content in TFL might have led to the lake's higher C absorption compared to YYL (Fig. 5).

3.3. The relationship between F_{CO2} and the limnological data

Chiu et al. (2020) showed that the DIC, DOC, and Chl. *a* are correlated with F_{CO2}. Overall, the DIC data that we obtained were associated with F_{CO2} in both YYL and TFL (Fig. 6a, b). The time series of water quality data and the SEM analysis showed that the DIC, DOC, Chl. *a*, and wind speed were also the predominant factors controlling F_{CO2} (Suppl. Figs. S2, S3). Specifically, F_{CO2} was significantly correlated with DIC in the during-typhoon period in both TFL and YYL ($R^2 > 0.9$, $p < 0.001$). DOC and F_{CO2} were positively correlated in TFL and YYL in the during-typhoon period but not in the YYL pre-typhoon or post-typhoon periods (Fig. 6c, d).

In addition, Chl. *a* had a slightly negative correlation with F_{CO2} in TFL but not in YYL (Fig. 6e, f). The wind speed was negatively correlated with F_{CO2} in TFL (Fig. 6h). The wind speed was not associated with F_{CO2} in YYL because it (0.11 m s^{-1}–2.72 m s^{-1}) was less than half of the wind speed in TFL (0.58–3.89 m s^{-1}) (Fig. 6g, h). The average t_r of TFL was 22.3 d, which is longer than the 5.30 d of YYL (Table 1).

3.4. The effects of a typhoon on the C flux

To clarify how typhoons affect DIC, we investigated the influence of Typhoon Megi (No. 1617; September 26–29, 2016), the strongest typhoon that occurred in Taiwan during the years from 2009 to 2017 (Typhoon database of the Central Weather Bureau of Taiwan, https://rdc28.cwb.gov.tw/TDB/). Our analyses revealed that typhoons induced a vertical mixing of lake waters and thus temporarily decreased the DIC level. The maximum PAR reaches 2000 μmol photons m^{-2} s^{-1} on normal days, but during Typhoon Megi, the max. PAR decreased to 300–500 μmol photons m^{-2} s^{-1} (Fig. 7a, b). The PAR even reached close to zero in the middle of Typhoon Megi (September 28). The water columns were well mixed during two days of the typhoon (Fig. 7c, d).

After Typhoon Megi passed, the vertical gradient of water temperature was approx. 1.50 °C m^{-1} in YYL and 0.50 °C m^{-1} in TFL from September 29 to October 1, 2016 (Fig. 7c, d). The stratification recovered to its original level (>2.0 °C m^{-1}) after October 2. The wind speeds at YYL and TFL are relatively lower than those of other low-altitude lakes, resulting in stable stratification. A typhoon mixes entire water columns within 1 week in YYL and TFL. The stratification is thus solid in both lakes from April to September. The Chl. *a* values of the lakes increased temporarily due to the nutrient inflow from rivers (Fig. 7e, f), and the wind speed and precipitation dramatically increased from September 26th to 28th (Fig. 7g, h). In addition, the precipitation was around 369–583 mm d-1 (Fig. 7i, j), which contributed 10.0%–11.1% of the annual precipitation at the measurement sites. After Typhoon Megi, the CDOM was diluted by 50.0% in YYL and approached 0.0 ppb (QSE) in TFL (Fig. 7e, f).

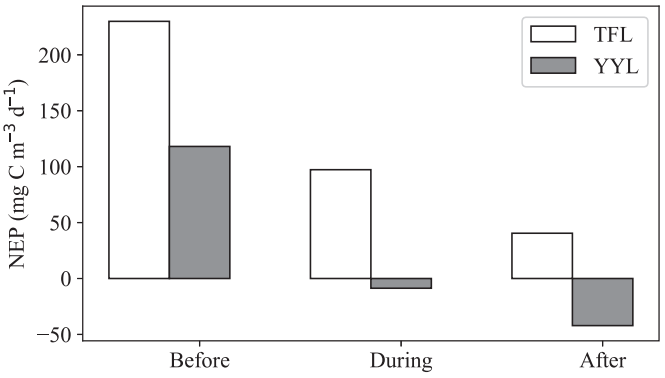

Fig. 5. The average NEP (mg C m^{-3} d^{-1}) between YYL (*gray bars*) and TFL (*white bars*) for each period (pre-typhoon, during typhoon, and posttyphoons).

Table 1
Residence times (t_r) during the three typhoon-related periods.

Site	Period		
Parameters	Before-typhoon	During-typhoon	After-typhoon
Yuang-Yang Lake (YYL)			
Volume, m^3	4.10 × 10^4	4.29 × 10^4	4.02 × 10^4
Discharge, m^3 s^{-1}	0.048	0.107	0.028
Water depth, m	4.38	4.46	4.35
t_r′[a], d	9.86	4.64	16.6
t_r, d	5.8	4.4	5.7
Overestimate, by t_r′, %	70.1	5.45	191
Tsui-Fong Lake (TFL)			
Volume, m^3	2.19 × 10^5	8.32 × 10^5	3.39 × 10^5
Discharge, m^3 s^{-1}	0.185	0.411	0.067
Water depth, m	3.27	7.01	4.08
t_r ′ *, d	13.7	23.4	58.6
t_r,d	10	18	39
Overestimate, by t_r′, %	37	30.2	50.2

[a] t_r′ shows the watershed area to lake volume ratio.

4. Discussion

Our results demonstrated that typhoon-induced mixing is a critical process determining the seasonal patterns of water quality (DIC, DOC, and Chl. *a*) and their effect on the C flux and NEP in shallow subtropical lakes (Figs. 2–5). The NEP decreased in the during- and post-typhoon periods because typhoon disturbances and external C-loading via rivers control the vertical distribution of C in lakes (Fig. 5). Our numerical simulations revealed that the average t_r values were 5.30 and 22.3 d in YYL and TFL, respectively, according to base flow, meaning that the hydraulic retention is significantly different between these two lakes (Table 1). The magnitude of t_r may also indicate that YYL and TFL had different regimes of ecosystem resilience (Table 1).

4.1. The hydraulic retention's effect on C flux in a stratified lake

According to previous studies, a two-layer assumption is acceptable for water quality analyses (Maruya et al., 2010; Nakayama et al., 2010; Sato et al., 2012). The longer the residence time, the greater the chemical transformations among the DIC, DOC, and phytoplankton growth, which results in a high correlation among pCO_2, DOC, and Chl. *a* due to photosynthesis/respiration (Carpenter et al., 1998; Sobek et al., 2003, 2005; Dodds and Whiles, 2020) and mineralization (Aarnos et al., 2018; Allesson et al., 2020). In addition, the residence time is a function of the total lake volume and river inflow. Our analysis of the effects of Typhoon Megi also showed that TFL had a longer t_r than YYL, even during a strong typhoon.

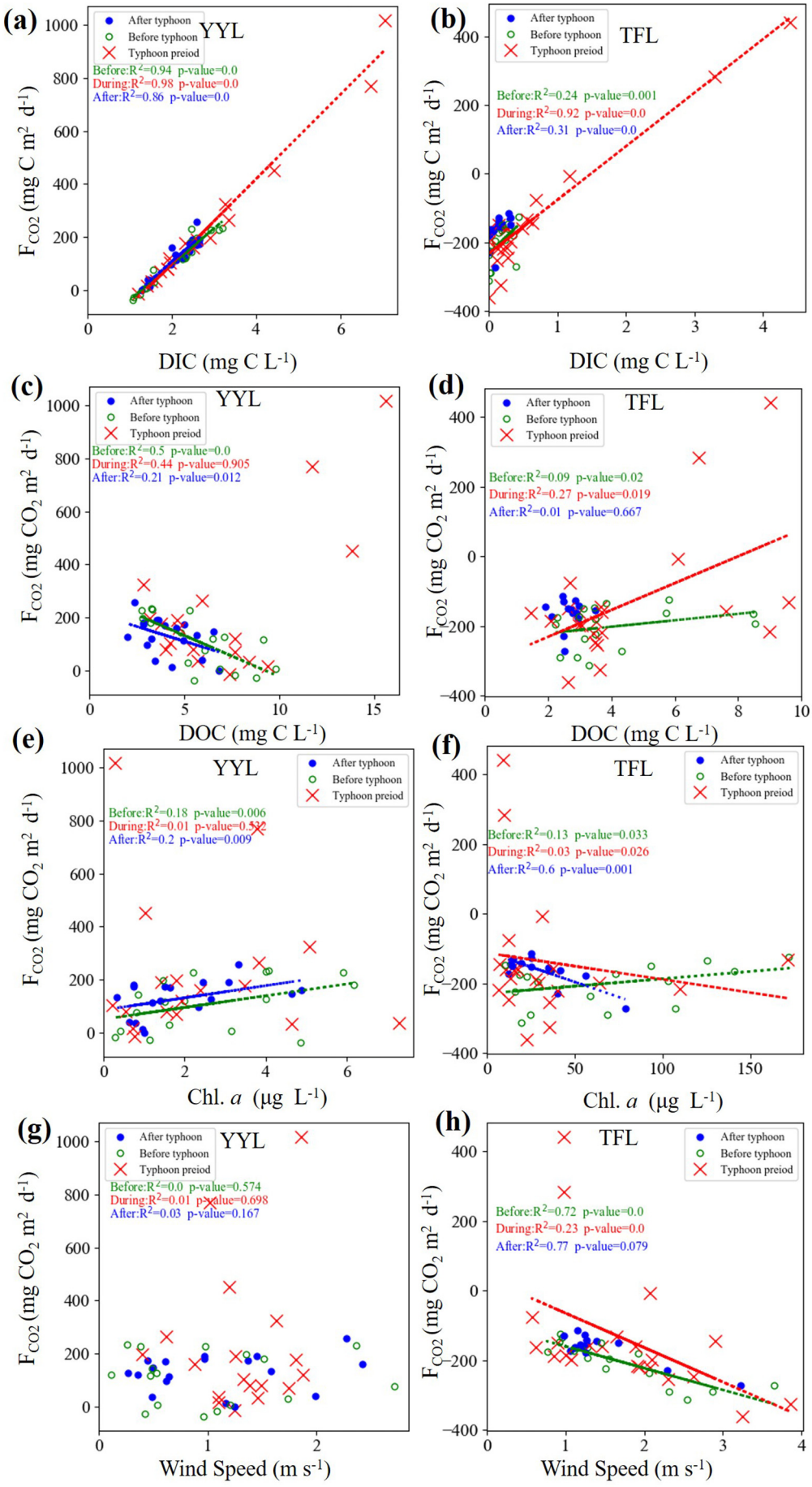
(a)
YYL
After typhoon
Before typhoon
Typhoon preiod
Before:R²=0.94 p-value=0.0
During:R²=0.98 p-value=0.0
After:R²=0.86 p-value=0.0
F_CO2 (mg C m² d⁻¹)
DIC (mg C L⁻¹)
(b)
TFL
Before:R²=0.24 p-value=0.001
During:R²=0.92 p-value=0.0
After:R²=0.31 p-value=0.0
(c)
YYL
Before:R²=0.5 p-value=0.0
During:R²=0.44 p-value=0.905
After:R²=0.21 p-value=0.012
F_CO2 (mg CO2 m² d⁻¹)
DOC (mg C L⁻¹)
(d)
TFL
Before:R²=0.09 p-value=0.02
During:R²=0.27 p-value=0.019
After:R²=0.01 p-value=0.667
(e)
YYL
Before:R²=0.18 p-value=0.006
During:R²=0.01 p-value=0.532
After:R²=0.2 p-value=0.009
Chl. a (μg L⁻¹)
(f)
TFL
Before:R²=0.13 p-value=0.033
During:R²=0.03 p-value=0.026
After:R²=0.6 p-value=0.001
(g)
YYL
Before:R²=0.0 p-value=0.574
During:R²=0.01 p-value=0.698
After:R²=0.03 p-value=0.167
Wind Speed (m s⁻¹)
(h)
TFL
Before:R²=0.72 p-value=0.0
During:R²=0.23 p-value=0.0
After:R²=0.77 p-value=0.079

Several research groups have reported that the residence time needs to be >1 week for phytoplankton and planktic bacteria to grow after storm events (Padisák, 1993; Shade et al., 2011; Jennings et al., 2012; Chiu et al., 2020). Our present SEM analysis results also support our hypothesis (Suppl. Fig. S3) that Chl. *a* is one of the significant factors controlling F_{CO2}. It is thus necessary to clarify the physical processes that are needed to estimate theF_{CO2} in a lake (such as hydraulic retention) considering the photosynthesis effect due to phytoplankton (Nakayama et al., 2020b).

Figs. 2b and 3b show that the strength of stratification varied considerably, indicating that a model can be applied in not only a stratified lake but also a well-mixed lake. Our two-layer model covers the vertical flux between the upper and lower layers with entrainment velocities and the intrusion of river inflow into both the upper and lower layers. The two-layer model used in this study thus provides a significant advantage for analyzing a weakly stratified lake, even a one-layer system, by giving large entrainment velocity and inflow into the lower layer in Eq. (S6) (Suppl. File S2).

Note that the total water depth was greater than the thermistor chain (3.50 m) in TFL and the water temperatures under 3.50 m in the hypolimnion were not measured, which suggests that the stratification strength estimated from Fig. 3b is weaker than the actual strength. In addition, the Wedderburn number and Lake number were confirmed to be large enough to not cause upwelling and turnover on normal days in TFL, even though the wind speed's effect is more significant on TFL than YYL, and thus stronger wind does not result in the occurrence of weak stratification (Imberger and Patterson, 1990; Shintani et al., 2011). The Wedderburn number is the parameter that inversely shows the magnitude of the upwelling scale. The Lake number is the parameter used to predict a modal-type response, such as the turnover in a whole lake.

The theoretical residence time, t_r' (Eq. (S7)), tended to overestimate the actual t_r that we obtained using Fantom, as Table 1 shows. For example, the simulated t_r was 39.0 d during the post-typhoon period in TFL, but the t_r' estimated by using the river inflow was 58.6 d. The t_r' overestimates by approx. 5.5%–191% if the stratification is ignored in the whole lake based on a 3D numerical model. We thus recommend computing the residence time by using a 3D hydrological model. Although the NEP obtained by Eq. (11) uses the epilimnion DIC and F_{CO2}, Eq. (S6) (Suppl. 2) revealed that Eq. (11) indeed includes the DIC flux from the lake bottom within the entire lake. Therefore, Eq. (11) is sufficiently accurate to estimate the NEP in an entire lake, even a stratified one.

Moreover, the general circulation model can predict future changes in the discharge and residence time under projected precipitation variations. Eq. (11) is thus promising to predict the long-term DIC variation in a subtropical shallow lake under the circumstances of climate change. We can also forecast the effects of global warming on the C flux in a lake if a long-term meteorological dataset is available, for example, from 1990 to 2010. Even a dataset from 2000 to 2020 may assist in investigating the effect of climate change on the C flux in a lake.

4.2. Comparison of the F_{CO2} between lakes during storm events

We chose to compare the F_{CO2} in the two lakes YYL and TFL with the shallow lakes from previous studies during storms in different climate zones (Table 2). Overall, F_{CO2} increased during the post-storm period. F_{CO2} increased by 48%–694% during the post-storm period in oligotrophic lakes (Table 2). Our present findings demonstrated that the fall overturn is a crucial process for mixing the water column, resulting in an increase in the F_{CO2} after summer storms (Vachon and del Giorgio, 2014; Czikowsky et al., 2018). The present results demonstrated that the post-storm period had the most considerable standard deviation, 323 mg CO_2 m^{-2} d^{-1}, due to the intense precipitation (the max. rainfall was 678 mm $time^{-1}$ for the 2016 Typhoon Megi, Fig. 7i, j), strong winds (the max. U_{10} was 30 m s^{-1} for the same typhoon, Fig. 11g, h), and short residence time (t_r') (Table 2).

Zwart et al. (2017) suggested that the t_r' was not only related to the water renewal rate (hydraulic retention) but also negatively associated with the terrestrial DOC (tDOC) during extreme rainstorms, which may induce the increase in F_{CO2} during the post-storm period (Table 2). The colored dissolved organic matter (CDOM) is a proxy for tDOM inputs, affecting the seasonal dynamics of underwater light, thermal stratification, nutrients, and primary production in freshwater ecosystems (Thrane et al., 2014; Fichot et al., 2016). Chiu et al. (2020) identified substantial CDOM and tDOM loads into both YYL and TFL, resulting in the amplification of F_{CO2} after strong typhoons. The previous studies investigated storm events with a max. rainfall of ~50 mm, which is less than the subtropical storm event examined by Kossin et al. (2013).

Autotrophic organisms contribute 10%–50% of the C flux in lakes due to respiration (Vachon et al., 2017). Our present results showed that aquatic production (photosynthesis), as inferred by Chl. *a*, was one of the most significant factors controlling DIC during the pre- and post-typhoon periods in TFL (Suppl. Fig. S3a, c). The Chl. *a* rapidly returned to its original level the next day after Typhoon Megi (Fig. 7f). The DOC and phosphorus (P) are critical factors determining the trophic state and primary production in shallow lakes (Hanson et al., 2003; Tsai et al., 2008). In previous studies of TDL, the TP was associated with the algae biomass (Tsai et al., 2016; Chiu et al., 2020), which may enhance the positive NEP from pre- to post-typhoon periods in a shallow mesotrophic lake such as TFL (Fig. 5, Table 2). Conversely, YYL depends on river discharge and allochthonous and autochthonous DOC loads (Tsai et al., 2008; Chiu et al., 2020; Suppl. Fig. S2). In YYL, the planktic bacteria composition changes during typhoon events (Shade et al., 2010, 2011), impacting ecological respiration. Hydraulic retention and typhoon disturbance thus play significant roles in the C flux patterns in YYL and TFL.

Lake and watershed morphometries may be a key to predicting the CO_2 flux in lakes after storm events (Klug et al., 2012; Vachon and del Giorgio, 2014). Klug et al. (2012) revealed that the ratio of the watershed area (WA) and lake volume (LV) (WA:LV) is correlated with typhoon disturbance; lakes with a high WA:LV ratio are more sensitive to storms compared to lakes with a low WA:LV value. In general, high WA:LV lakes tend to have higher lake water renewal rates during storm events (Klug et al., 2012; Vachon and del Giorgio, 2014). den Heyer and Kalff (1998) found that the higher the WA:LV, the shorter the t_r, resulting in lower mineralization rates.

In contrast, CO_2 dynamics with a low WA:LV ratio depend highly on internal production unless a strong typhoon comes (Klug et al., 2012; Table 2). The different responses of F_{CO2} during storms thus depend on lake and watershed morphometries such as the t_r and the storm's intensity (den Heyer and Kalff, 1998; Klug et al., 2012; Vachon and del Giorgio, 2014; Zwart et al., 2017). Our present analyses also revealed that the t_r and typhoons are also vital factors impacting the F_{CO2} in YYL and TFL.

4.3. C fluxes in shallow subtropical lakes

The absolute value of F_{CO2} is 96%–537% of the NEP in YYL and 42%–70% in TFL (Figs. 2f, 3f, 5). In general, the seasonal F_{CO2} (NEE) > NEP in these two lakes revealed that most of the C was degassed to the atmosphere from the sediment or the river inputs. CO_2 or the other forms of C could be brought into the lakes, contributing to the DIC level during rainy seasons by groundwater or surface flow (Vachon and del Giorgio, 2014; Chiu et al., 2020). Note that the NEE for an entire lake tends to be

Fig. 6. The relationship between F_{CO2} and limnological data (Wind speed (U_{10}), DIC, DOC, and Chl. *a* at the epilimnion (a, c, e, g) in YYL and (b, d, f, h) in TFL. *Green circles*: the pre-typhoon period. *Red crosses*: the during-typhoon period. *Blue dots*: the post-typhoon period. The *dotted lines* represent the linear regression line for each period. (For interpretation of the references to color in this figure legend, the reader is referred to the web version of this article.)

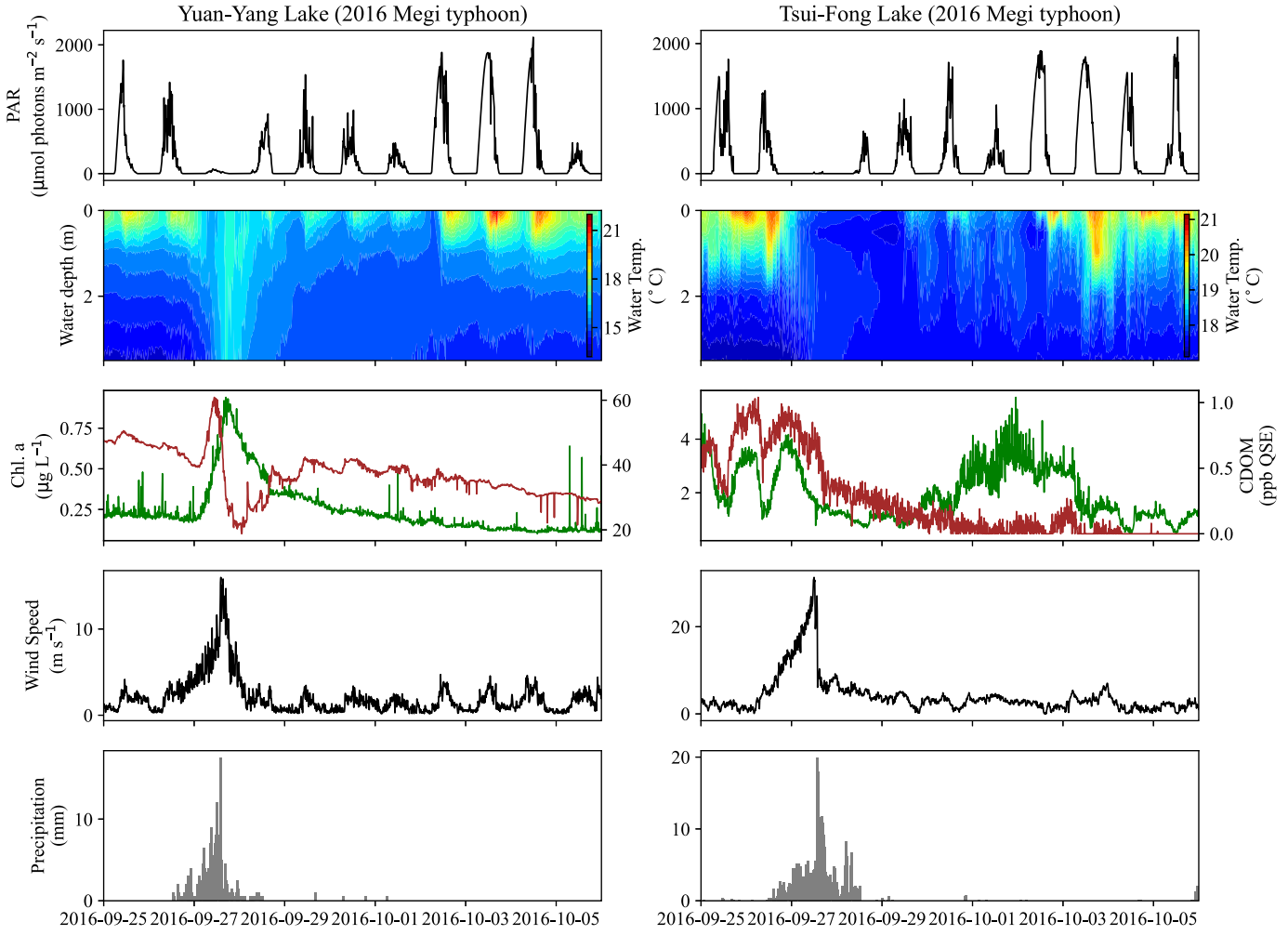

Fig. 7. Data profile of the (a, b) PAR, (c, d) water temperature, (e, f) Chl. *a* (*green line*) and CDOM (*brown line*) at 0.25 m water depth. g, h: Wind speed at 10 m high (U_{10}) and (i, j) precipitation in YYL and TFL during Typhoon Megi (September 25 to October 5, 2016). Data were captured every 10 min. (For interpretation of the references to color in this figure legend, the reader is referred to the web version of this article.)

smaller than the NEP in a stratified lake when the organic matter production and respiration are predominant in the ecosystem, and the NEP is >0 although the NEE for the entire lake should be the same as the NEP if there is no stratification (see Suppl. File 2 for details).

In addition, the wind speed is one of the most significant parameters influencing the F_{CO2} (Eqs. (8), (9)). Czikowsky et al. (2018) showed that the wind speed is negatively correlated with the F_{CO2} when $U_{10} < 4.0$ m s^{-1} in a stratified temperate lake, similar to our findings for TFL (Suppl. Figs. S2, 6g). However, the wind speed at YYL was not associated with the F_{CO2}, because the wind speed was low (0.11 m s^{-1}–2.72 m s^{-1}) (Fig. 6h). The SEM analysis results showed that mineralization might be an important process for DIC

Table 2
Comparison of the F_{CO2} (mg CO_2 m^{-2} d^{-1}) in several shallow lakes (average water depth < 15 m) during post-storm events.

Lake site	Location	Climate zone	Trophic state	Lake area, km^2	Avg. depth, m	WA: LV[a]	Avg. t_r', d	Avg. F_{CO2} (SD)	Avg. F_{CO2} post-storm (SD)	Storm rainfall, mm time^{-1}	Max. U_{10}, m s^{-1}	Reference
Nhecolândia, Brazil	15°–22°S, 55°–60°W	Tropical	Oligo. (Black)	0.087–0.093	~0.5	–	–	102.5	–	–	–	Barbiero et al., 2018
			Meso. or Eutrophic (Green)	0.053-0.285		–	–	−229	~−110	150	–	
Yuang-Yang, Taiwan	24.58° N, 121.40° E	Subtropical	Oligo. (humic)	0.035	4.4	3.37	10.4	145 (100)	210.5 (323)	330–678	8–15	This study
Tsui-Fong, Taiwan	24.52° N, 121.60° E	Subtropical	Meso.	0.08–0.25	4.8	4.2–15.5	31.9	−165.1 (55.2)	−96.5 (223)	330–678	10–30	This study
Pleasant, USA	43.48° N, 74.38° W	Temperate	Oligo.	6.0	8.0	–	–	276	342	–	8.0	Czikowsky et al., 2018
Croche, Canada	45.99° N, 74.00° W	Temperate	Oligo.	0.063	6.0	0.95	170	88.7 (36.8)	616 (209)	30–50	4.0	Vachon and del Giorgio, 2014
Simoncouche, Canada	48.23° N, 71.25° W	Temperate	Oligo.	0.861	2.1	14.6	50	107.8 (65.7)	458.1 (181)	20–30	4.0	Vachon and del Giorgio, 2014

[a] The watershed area-to-lake volume ratio.

and the F_{CO2} (Suppl. Figs. S2, S3). den Heyer and Kalff (1998) showed that the organic matter and C mineralization at the water surface were three times higher than the sediment C emission. Our present findings showed that photo-mineralization was not associated with DIC (Suppl. Figs. S2, S3). In contrast to the linear regression, the SEM analysis showed that the correlation among pCO_2, DOC, and Chl. *a* was higher in TFL than YYL, suggesting that an SEM analysis is more suitable for analyzing such correlations than a one-to-one linear regression analysis.

This study revealed that the hydraulic retention effect is critical for accurately estimating the NEP in a stratified lake. Vertical mixing is a crucial physical process that decides the seasonal dynamics of the C flux in shallow subtropical lakes (Chiu et al., 2020; Lin et al., 2021). However, other processes may affect the C flux in lakes, such as C burial and sedimentation (Cole et al., 2007; Mendonça et al., 2017; Bartosiewicz et al., 2019). Mendonça et al. (2017) demonstrated that the organic C burial in sediment was 38.4–101 mg of C m^{-2} d^{-1}, contributing approx. 20%–40% of the F_{CO2} in global lakes (Cole et al., 2007; Raymond et al., 2013). C burial has a dramatic effect primarily in strong thermal stratified lakes (Bartosiewicz et al., 2019) because the CDOC and CDOM rapidly increase via terrestrial DOC (tDOC) after extreme storm events (Read and Rose, 2013; Chiu et al., 2020). Our present results demonstrated that the CDOM became diluted by 30%–50% after Typhoon Megi (Fig. 7e, f).

CDOM and tDOM are vital drivers that regulate metabolism and C flux in lakes (Staehr et al., 2010; Lapierre et al., 2013; Chiu et al., 2020), and this resulted in the dramatic decrease in the NEP during the strong typhoon in this study (Fig. 5). The particulate organic C (POC) and DOC comprise 10%–50% of total C fluxes in a lake ecosystem (Hope et al., 1994; Tranvik et al., 2009; Hanson et al., 2015), and allochthonous and autochthonous C comes mostly from tDOC and terrestrial POC (Tranvik et al., 2009; Hanson et al., 2011, 2015). The external C load contributes 20%–50% of the C flux into lakes (Vachon et al., 2017). A future research focus is the investigation of the organic C load, mineralization rates, and C burial in sediment during typhoons to clarify the fate of total C fluxes in shallow subtropical lakes. This knowledge could help us understand the total C fluxes' internal resilience and modulation under extreme weather events in a lake ecosystem. From the viewpoint of biochemical and biophysical research, we suggest that a stable isotope analysis is necessary to clarify the contributions of DOC and C from the lake bottom on the C flux.

5. Conclusions

We investigated the hydraulic retention effect and typhoon disturbance impact on the C flux in two subtropical shallow lakes in Taiwan. We used a 3D numerical model (Fantom) to calculate the residence time t_r for evaluating the hydraulic retention effect. The NEP in Yuang-Yang Lake (YYL) decreased by 107%–136% in the during- and post-typhoon periods because inflow rapidly refreshes the lake water (the t_r was 4.4 d). In contrast, the NEP in Tsui-Fong Lake (TFL) decreased by 57.6%–82.3% in the during- and post-typhoon periods because of the relatively longer t_r of 39.0 d. The typhoon-induced mixing was therefore a critical physical phenomenon affecting the C flux in two lakes with different trophic levels. We also observed that the NEP decreased by 160 mg C m^{-3} d^{-1} in YYL and 190 mg C m^{-3} d^{-1} in TFL from the pre-typhoon to post-typhoon periods because of the different trophic states. This study has thus characterized the seasonal patterns of C flux in a subtropical shallow lake due to typhoon disturbances considering the hydraulic retention effect.

Supplementary data to this article can be found online at https://doi.org/10.1016/j.scitotenv.2021.150044.

CRediT authorship contribution statement

Hao-Chi Lin: Conceptualization, Methodology, Investigation, Formal analysis, Writing – original draft. **Jeng-Wei Tsai:** Investigation, Writing – review & editing. **Kazufumi Tada:** Software, Writing – review & editing. **Hiroki Matsumoto:** Software, Writing – review & editing. **Chih-Yu Chiu:** Funding acquisition, Writing – review & editing. **Keisuke Nakayama:** Methodology, Software, Supervision, Writing – review & editing, Conceptualization, Investigation, Formal analysis.

Declaration of competing interest

The authors declared that they have no competing interests.

Acknowledgments

This work was supported by the Ministry of Science and Technology, Taiwan (MOST 105-2621-B-039-001, MOST 107-2621-M-239-001), Academia Sinica, Taiwan (AS-103-TP-B15) to C.Y. Chiu; China Medical University (CMU108-S-26 and CMU109-S-16) to J.W. Tsai; and the Japan Society for the Promotion of Science (grants 18H01545 and 18KK0119) to K. Nakayama. We thank J.Y. Liu, Y.X. Lan, Z.Y. Wu, Y.J. Miao, and L.C. Jiang for assisting with water sample collection and chemical analysis. This study benefited from participation in the Global Lakes Ecological Observatory Network (GLEON).

References

Aarnos, H., Gélinas, Y., Kasurinen, V., Gu, Y., Puupponen, V.M., Vähätalo, A.V., 2018. Photochemical mineralization of terrigenous DOC to dissolved inorganic carbon in ocean. Glob. Biogeochem. Cycl. 32 (2), 250–266. https://doi.org/10.1002/2017GB005698.

Adcroft, A., Hill, C., Marshall, J., 1997. Representation of topography by shaved cells in a height coordinate ocean model. Mon. Wea. Rev. 125 (9), 2293–2315. https://doi.org/10.1175/1520-0493(1997)125<2293:ROTBSC>2.0.CO;2.

Allesson, L., Koehler, B., Thrane, J.E., Andersen, T., Hessen, D.O., 2020. The role of photomineralization for CO2 emissions in boreal lakes along a gradient of dissolved organic matter. Limnol. Oceanogr. 9999, 1–13. https://doi.org/10.1002/lno.11594.

Anesio, A.M., Granéli, W., 2003. Increased photoreactivity of DOC by acidification: implications for the carbon cycle in humic lakes. Limnol. Oceanogr. 48 (2), 735–744. https://doi.org/10.4319/lo.2003.48.2.0735.

Bade, D.L., Carpenter, S.R., Cole, J.J., Hanson, P.C., Hesslein, R.H., 2004. Controls of d13C-DIC in lakes: geochemistry, lake metabolism, and morphometry. Limnol. Oceanogr. 49 (4), 1160–1172. https://doi.org/10.4319/lo.2004.49.4.1160.

Barbiero, L., Neto, M.S., Braz, R.R., Do Carmo, J.B., Rezende Filho, A.T., Mazzi, E., Fernandes, F.A., Damatto, S.R., de Camargo, P.B., 2018. Biogeochemical diversity, O2-supersaturation and hot moments of GHG emissions from shallow alkaline lakes in the pantanal of Nhecolândia, Brazil. Sci. Total Environ. 619, 1420–1430. https://doi.org/10.1016/j.scitotenv.2017.11.197.

Bartosiewicz, M., Przytulska, A., Lapierre, J.F., Laurion, I., Lehmann, M.F., Maranger, R., 2019. Hot tops, cold bottoms: synergistic climate warming and shielding effects increase carbon burial in lakes. Limnol. Oceanogr. Lett. 4 (5), 132–144. https://doi.org/10.1002/lol2.10117.

Cai, W.J., Wang, Y., 1998. The chemistry, fluxes, and sources of carbon dioxide in the estuarine waters of the Satilla and Altamaha Rivers, Georgia. Limnol. Oceanogr. 43 (4), 657–668. https://doi.org/10.4319/lo.1998.43.4.0657.

Carpenter, S.R., Cole, J.J., Kitchell, J.F., Pace, M.L., 1998. Impact of dissolved organic carbon, phosphorus, and grazing on phytoplankton biomass and production in experimental lakes. Limnol. Oceanogr. 43 (1), 73–80. https://doi.org/10.4319/lo.1998.43.1.0073.

Chiu, C.Y., Jones, J.R., Rusak, J.A., Lin, H.C., Nakayama, K., Kratz, T.K., Liu, W.C., Tang, S.L., Tsai, J.W., 2020. Terrestrial loads of dissolved organic matter drive inter-annual carbon flux in subtropical lakes during times of drought. Sci. Total Environ. 717, 137052. https://doi.org/10.1016/j.scitotenv.2020.137052.

Cole, J.J., Caraco, N.F., 1998. Atmospheric exchange of carbon dioxide in a low-wind oligotrophic lake measured by the addition of SF6. Limnol. Oceanogr. 43 (4), 647–656. https://doi.org/10.4319/lo.1998.43.4.0647.

Cole, J.J., Prairie, Y.T., Caraco, N.F., McDowell, W.H., Tranvik, L.J., Striegl, R.G., Duarte, C.M., Kortelainen, P., Downing, J.A., Middelburg, J.J., Melack, J., 2007. Plumbing the global carbon cycle: integrating inland waters into the terrestrial carbon budget. Ecosystems 10 (1), 171–184. https://doi.org/10.1007/s10021-006-9013-8.

Czikowsky, M.J., MacIntyre, S., Tedford, E.W., Vidal, J., Miller, M.D., 2018. Effects of wind and buoyancy on carbon dioxide distribution and air-water flux of a stratified temperate lake. J. Geophy Res. Biogeosci. 123 (8), 2305–2322. https://doi.org/10.1029/2017JG004209.

den Heyer, C., Kalff, J., 1998. Organic matter mineralization rates in sediments: a within- and among-lake study. Limnol. Oceanogr. 43 (4), 695–705. https://doi.org/10.4319/lo.1998.43.4.0695.

Dodds, W., Whiles, M., 2020. Freshwater Ecology: Concepts and Environmental Applications of Limnology, third ed. Academic Press, London, pp. 749–752.

Fichot, C.G., Benner, R., Kaiser, K., Shen, Y., Amon, R.M.W., Ogawa, H., Lu, C.J., 2016. Predicting dissolved lignin phenol concentrations in the coastal ocean from chromophoric dissolved organic matter (CDOM) absorption coefficients. Front. Mar. Sci. 3, 7. https://doi.org/10.3389/fmars.2016.00007.

Groeneveld, M., Tranvik, L., Natchimuthu, S., Koehler, B., 2016. Photochemical mineralisation in a boreal brown water lake: considerable temporal variability and minor contribution to carbon dioxide production. Biogeosciences 13 (13), 3931–3943. https://doi.org/10.5194/bg-13-3931-2016.

Hanson, P.C., Bade, D.L., Carpenter, S.R., Kratz, T.K., 2003. Lake metabolism: relationships with dissolved organic carbon and phosphorus. Limnol. Oceanogr. 48 (3), 1112–1119. https://doi.org/10.4319/lo.2003.48.3.1112.

Hanson, P.C., Hamilton, D.P., Stanley, E.H., Preston, N., Langman, O.C., Kara, E.L., 2011. Fate of allochthonous dissolved organic carbon in lakes: a quantitative approach. PLOS ONE 6 (7), e21884. https://doi.org/10.1371/journal.pone.0021884.

Hanson, P.C., Pace, M.L., Carpenter, S.R., Cole, J.J., Stanley, E.H., 2015. Integrating landscape carbon cycling: research needs for resolving organic carbon budgets of lakes. Ecosystems 18 (3), 363–375. https://doi.org/10.1007/s10021-014-9826-9.

Hope, D., Billett, M.F., Cresser, M.S., 1994. A review of the export of carbon in river water: fluxes and processes. Environ. Pollut. 84 (3), 301–324. https://doi.org/10.1016/0269-7491(94)90142-2.

Hope, D., Kratz, T.K., Riera, J.L., 1996. Relationship between and dissolved organic carbon in northern Wisconsin lakes. J. Environ. Qual. 25 (6), 1442–1445. https://doi.org/10.2134/jeq1996.00472425002500060039x.

Imberger, J., Patterson, J.C., 1990. Physical limnology. Adv. Appl. Mech. 27, 303–473. https://doi.org/10.1016/S0065-2156(08)70199-6.

Jähne, B., Münnich, K.O., Bösinger, R., Dutzi, A., Huber, W., Libner, P., 1987. On the parameters influencing air-water gas exchange. J. Geophys. Res. Oceans 92 (C2), 1937–1949. https://doi.org/10.1029/JC092iC02p01937.

Jennings, E., Jones, S., Arvola, L., Staehr, P.A., Gaiser, E., Jones, I.D., Weathers, K.C., Weyhenmeyer, G.A., Chiu, C.Y., de Eyto, E., 2012. Effects of weather-related episodic events in lakes: an analysis based on high-frequency data. Fresh. Biol. 57 (3), 589–601. https://doi.org/10.1111/j.1365-2427.2011.02729.x.

Jones, W.P., Launder, B.E., 1972. The prediction of laminarization with a two-equation model of turbulence. J. Heat Mass Transf. 15 (2), 301–314. https://doi.org/10.1016/0017-9310(72)90076-2.

Jones, S.E., Kratz, T.K., Chiu, C.Y., McMahon, K.D., 2009. Influence of typhoons on annual CO2 flux from a subtropical, humic lake. Glob. Change Biol. 15 (1), 243–254. https://doi.org/10.1111/j.1365-2486.2008.01723.x.

Kimura, N., Liu, W.C., Chiu, C.Y., Kratz, T., 2012. The influences of typhoon-induced mixing in a shallow lake. Lakes Res. Res. Manag. 17 (3), 171–183. https://doi.org/10.1111/j.1440-1770.2012.00509.x.

Kimura, N., Liu, W.C., Chiu, C.Y., Kratz, T.K., 2014. Assessing the effects of severe rainstorm-induced mixing on a subtropical, subalpine lake. Environ. Monit. Assess. 186 (5), 3091–3114. https://doi.org/10.1007/s10661-013-3603-7.

Kimura, N., Liu, W.C., Tsai, J.W., Chiu, C.Y., Kratz, T.K., Tai, A., 2017. Contribution of extreme meteorological forcing to vertical mixing in a small, shallow subtropical lake. J. Limnol. 76 (1), 116–128. https://doi.org/10.4081/jlimnol.2016.1477.

Klug, J.L., Richardson, D.C., Ewing, H.A., Hargreaves, B.R., Samal, N.R., Vachon, D., Weathers, K.C., 2012. Ecosystem effects of a tropical cyclone on a network of lakes in northeastern North America. Environ. Sci. Technol. 46 (21), 11693–11701. https://doi.org/10.1021/es302063v.

Kossin, J.P., Olander, T.L., Knapp, K.R., 2013. Trend analysis with a new global record of tropical cyclone intensity. J. Clim. 26 (24), 9960–9976. https://doi.org/10.1175/JCLI-D-13-00262.1.

Lai, I.L., Chang, S.C., Lin, P.H., Chou, C.H., Wu, J.T., 2006. Climatic characteristics of the subtropical mountainous cloud forest at the Yuanyang Lake long-term ecological research site, Taiwan. Taiwania 51 (4), 317–329. https://doi.org/10.6165/tai.2006.51(4).317.

Lapierre, J.F., Guillemette, F., Berggren, M., Del Giorgio, P.A., 2013. Increases in terrestrially derived carbon stimulate organic carbon processing and CO2 emissions in boreal aquatic ecosystems. Nat. Commun. 4 (1), 1–7. https://doi.org/10.1038/ncomms3972.

Lin, H.C., Chiu, C.Y., Tsai, J.W., Liu, W.C., Tada, K., Nakayama, K., 2021. Influence of thermal stratification on seasonal net ecosystem production and dissolved inorganic carbon in a shallow subtropical lake. J. Geophy Res. Biogeosci. 126, e2020JG005907. https://doi.org/10.1029/2020JG005907.

MacIntyre, S., Crowe, A.T., Cortés, A., Arneborg, L., 2018. Turbulence in a small arctic pond. Limnol. Oceanogr. 63 (6), 2337–2358. https://doi.org/10.1002/lno.10941.

Maruya, Y., Nakayama, K., Shintani, T., Yonemoto, M., 2010. Evaluation of entrainment velocity induced by wind stress in a two-layer system. Hydrol. Res. Lett. 4, 70–74. https://doi.org/10.3178/hrl.4.70.

McDonald, C.P., Stets, E.G., Striegl, R.G., Butman, D., 2013. Inorganic carbon loading as a primary driver of dissolved carbon dioxide concentrations in the lakes and reservoirs of the contiguous United States. Glob. Biogeochem. Cycl. 27 (2), 285–295. https://doi.org/10.1002/gbc.20032.

Mendonça, R., Müller, R.A., Clow, D., Verpoorter, C., Raymond, P., Tranvik, L.J., Sobek, S., 2017. Organic carbon burial in global lakes and reservoirs. Nat. Commun. 8 (1), 1–7. https://doi.org/10.1038/s41467-017-01789-6.

Nakamoto, A., Nakayama, K., Shintani, T., Maruya, Y., Komai, K., Ishida, T., Makiguchi, Y., 2013. Adaptive management in Kushiro wetland in the context of salt wedge intrusion due to sea level rise. Hydrol. Res. Lett. 7 (1), 1–5. https://doi.org/10.3178/hrl.7.1.

Nakayama, K., Sivapalan, M., Sato, C., Furukawa, K., 2010. Stochastic characterization of the onset of and recovery from hypoxia in Tokyo Bay, Japan: derived distribution analysis based on "strong wind" events. Water Resour. Res. 46, W12532. https://doi.org/10.1029/2009WR008900.

Nakayama, K., Shintani, T., Shimizu, K., Okada, T., Hinata, H., Komai, K., 2014. Horizontal and residual circulations driven by wind stress curl in Tokyo Bay. J. Geophys. Res. Oceans 119 (3), 1977–1992. https://doi.org/10.1029/2020JC016120.

Nakayama, K., Nguyen, D.H., Shintani, T., Komai, K., 2016. Reversal of secondary flows in a sharp channel bend. Coast. Eng. J. 58 (02), 1650002. https://doi.org/10.1142/S0578563416500029.

Nakayama, K., Komai, K., Tada, K., Lin, H.C., Yajima, H., Yano, S., Hipsey, M.R., Tsai, J.W., 2020a. Modeling dissolved inorganic carbon considering submerged aquatic vegetation. Ecol. Model. 431 (1), 109188. https://doi.org/10.1016/j.ecolmodel.2020.109188.

Nakayama, K., Shintani, T., Komai, K., Nakagawa, Y., Tsai, J.W., Sasaki, D., Tada, K., Moki, H., Kuwae, T., Watanabe, K., Hipsey, M.R., 2020b. Integration of submerged aquatic vegetation motion within hydrodynamic models. Water Resour. Res. 56 (8), e2020WR027369. https://doi.org/10.1029/2020WR027369.

Ojala, A., Bellido, J.L., Tulonen, T., Kankaala, P., Huotari, J., 2011. Carbon gas fluxes from a brown-water and a clear-water lake in the boreal zone during a summer with extreme rain events. Limnol. Oceanogr. 56 (1), 61–76. https://doi.org/10.4319/lo.2011.56.1.0061.

Padisák, J., 1993. The influence of different disturbance frequencies on the species richness, diversity and equitability of phytoplankton in shallow lakes. Hydrobiologia 249 (1), 135–156. https://doi.org/10.1007/BF00008850.

Plummer, L.N., Busenberg, E., 1982. The solubilities of calcite, aragonite and vaterite in CO2-H2O solutions between 0 and 90°C, and an evaluation of the aqueous model for the system CaCO3-CO2-H2O. Geochem. Cosmochimica Acta. 46 (6), 1011–1040. https://doi.org/10.1016/0016-7037(82)90056-4.

Raymond, P.A., Hartmann, J., Lauerwald, R., Sobek, S., McDonald, C., Hoover, M., Guth, P., 2013. Global carbon dioxide emissions from inland waters. Nature 503 (7476), 355–359. https://doi.org/10.1038/nature12760.

Read, J.S., Rose, K.C., 2013. Physical responses of small temperate lakes to variation in dissolved organic carbon concentrations. Limnol. Oceanogr. 58 (3), 921–931. https://doi.org/10.4319/lo.2013.58.3.0921.

Rose, K.C., Winslow, L.A., Read, J.S., Hansen, G.J., 2016. Climate-induced warming of lakes can be either amplified or suppressed by trends in water clarity. Limnol. Oceanogr. Lett. 1 (1), 44–53. https://doi.org/10.1002/lol2.10027.

Sato, C., Nakayama, K., Furukawa, K., 2012. Contributions of wind and river effects on DO concentration in Tokyo Bay. Estuar. Coast. Shelf Sci. 109, 91–97. https://doi.org/10.1016/j.ecss.2012.05.023.

Schindler, D.W., Curtis, P.J., Parker, B.R., Stainton, M.P., 1996. Consequences of climate warming and lake acidification for UV-B penetration in north american boreal lakes. Nature 379 (6567), 705–708. https://doi.org/10.1038/379705a0.

Scully, N.M., McQueen, D.J., Lean, D.R.S., 1996. Hydrogen peroxide formation: the interaction of ultraviolet radiation and dissolved organic carbon in lake waters along a 43–75 N gradient. Limnol. Oceanogr. 41 (3), 540–548. https://doi.org/10.4319/lo.1996.41.3.0540.

Shade, A., Chiu, C.Y., McMahon, K.D., 2010. Seasonal and episodic lake mixing stimulate differential planktonic bacterial dynamics. Microb. Ecol. 59 (3), 546–554. https://doi.org/10.1007/s00248-009-9589-6.

Shade, A., Read, J.S., Welkie, D.G., Kratz, T.K., Wu, C.H., McMahon, K.D., 2011. Resistance, resilience and recovery: aquatic bacterial dynamics after water column disturbance. Environ. Microbiol. 13 (10), 2752–2767. https://doi.org/10.1111/j.1462-2920.2011.02546.x.

Shintani, T., De La Fuente, A., Niño, Y., Imberger, J., 2011. Generalizations of the Wedderburn number: parameterizing upwelling in stratified lakes. Limnol. Oceanogr. 55 (3), 1377–1389. https://doi.org/10.4319/lo.2010.55.3.1377.

Smith, S.V., 1985. Physical, chemical and biological characteristics of CO2 gas flux across the air-water interface. Plant Cell Environ. 8 (6), 387–398. https://doi.org/10.1111/j.1365-3040.1985.tb01674.x.

Sobek, S., Algesten, G., Bergström, A.K., Jansson, M., Tranvik, L.J., 2003. The catchment and climate regulation of pCO2 in boreal lakes. Glob. Chang. Biol. 9 (4), 630–641. https://doi.org/10.1046/j.1365-2486.2003.00619.x.

Sobek, S., Tranvik, L.J., Cole, J.J., 2005. Temperature independence of carbon dioxide supersaturation in global lakes. Glob. Biogeochem. Cycl. 19, GB2003. https://doi.org/10.1029/2004GB002264.

Sobek, S., Tranvik, L.J., Prairie, Y.T., Kortelainen, P., Cole, J.J., 2007. Patterns and regulation of dissolved organic carbon: an analysis of 7,500 widely distributed lakes. Limnol. Oceanogr. 52 (3), 1208–1219. https://doi.org/10.4319/lo.2007.52.3.1208.

Staehr, P.A., Sand-Jensen, K., Raun, A.L., Nilsson, B., Kidmose, J., 2010. Drivers of metabolism and net heterotrophy in contrasting lakes. Limnol. Oceanogr. 55 (2), 817–830. https://doi.org/10.4319/lo.2010.55.2.0817.

Striegl, R.G., Kortelainen, P., Chanton, J.P., Wickland, K.P., Bugna, G.C., Rantakari, M., 2001. Carbon dioxide partial pressure and 13C content of north temperate and boreal lakes at spring ice melt. Limnol. Oceanogr. 46, 941–945. https://doi.org/10.4319/lo.2001.46.4.0941.

Thrane, J.E., Hessen, D.O., Andersen, T., 2014. The absorption of light in lakes: negative impact of dissolved organic carbon on primary productivity. Ecosystems 17, 1040–1052. https://doi.org/10.1007/s10021-014-9776-2.

Tranvik, L.J., 1988. Availability of dissolved organic carbon for planktonic bacteria in oligotrophic lakes of differing humic content. Microb. Ecol. 16 (3), 311–322. https://doi.org/10.1007/bf02011702.

Tranvik, L.J., Downing, J.A., Cotner, J.B., Loiselle, S.A., Striegl, R.G., Ballatore, T.J., Weyhenmeyer, G.A., 2009. Lakes and reservoirs as regulators of carbon cycling and climate. Limnol. Oceanogr. 54 (part2), 2298–2314. https://doi.org/10.4319/lo.2009.54.6_part_2.2298.

Tsai, J.W., Kratz, T.K., Hanson, P.C., Wu, J.T., Chang, W.Y., Arzberger, P.W., Lin, B.S., Lin, F.P., Chou, H.M., Chiu, C.Y., 2008. Seasonal dynamics, typhoons and the regulation of lake metabolism in a subtropical humic lake. Fresh. Biol. 53 (10), 1929–1941. https://doi.org/10.1111/j.1365-2427.2008.02017.x.

Tsai, J.W., Kratz, T.K., Hanson, P.C., Kimura, N., Liu, W.C., Lin, F.P., Chou, H.M., Wu, J.T., Chiu, C.Y., 2011. Metabolic changes and the resistance and resilience of a subtropical heterotrophic lake to typhoon disturbance. Can. J. Fish. Aquat. Sci. 68 (5), 768–780. https://doi.org/10.1139/f2011-024.

Tsai, J.W., Kratz, T.K., Rusak, J.A., Shih, W.Y., Liu, W.C., Tang, S.L., Chiu, C.Y., 2016. Absence of winter and spring monsoon changes water level and rapidly shifts metabolism in a subtropical lake. Inland Waters 6 (3), 436–448. https://doi.org/10.1080/IW-6.3.844.
Umlauf, L., Burchard, H., 2003. A generic length-scale equation for geophysical turbulence models. J. Mar. Res. 61 (2), 235–265. https://doi.org/10.1357/002224003322005087.
Vachon, D., del Giorgio, P.A., 2014. Whole-lake CO2 dynamics in response to storm events in two morphologically different lakes. Ecosystems 17 (8), 1338–1353. https://doi.org/10.1007/s10021-014-9799-8.
Vachon, D., Solomon, C.T., del Giorgio, P.A., 2017. Reconstructing the seasonal dynamics and relative contribution of the major processes sustaining CO2 emissions in northern lakes. Limnol. Oceanogr. 62 (2), 706–722. https://doi.org/10.1002/lno.10454.
Wanninkhof, R., 1992. Relationship between wind speed and gas exchange over the ocean. J. Geophys. Res. Oceans. 97 (C5), 7373–7382. https://doi.org/10.1029/92JC00188.
Williamson, C.E., Morris, D.P., Pace, M.L., Olson, O.G., 1999. Dissolved organic carbon and nutrients as regulators of lake ecosystems: resurrection of a more integrated paradigm. Limnol. Oceanogr. 44 (3part2), 795–803. https://doi.org/10.4319/lo.1999.44.3_part_2.0795.
Williamson, C.E., Overholt, E.P., Pilla, R.M., Leach, T.H., Brentrup, J.A., Knoll, L.B., Mette, E.M., Moeller, R.E., 2015. Ecological consequences of long-term browning in lakes. Sci. Rep. 5, 18666. https://doi.org/10.1038/srep18666.
Woolway, R.I., Simpson, J.H., Spiby, D., Feuchtmayr, H., Powell, B., Maberly, S.C., 2018. Physical and chemical impacts of a major storm on a temperate lake: a taste of things to come? Clim. Chang. 151 (2), 333–347. https://doi.org/10.1007/s10584-018-2302-3.
Woolway, R.I., Kraemer, B.M., Lenters, J.D., Merchant, C.J., O'Reilly, C.M., Sharma, S., 2020. Global lake responses to climate change. Nat. Rev. Earth Environ. 1 (8), 388–403. https://doi.org/10.1038/s43017-020-0067-5.
Zwart, J.A., Sebestyen, S.D., Solomon, C.T., Jones, S.E., 2017. The influence of hydrologic residence time on lake carbon cycling dynamics following extreme precipitation events. Ecosystems 20 (5), 1000–1014. https://doi.org/10.1007/s10021-016-0088-6.